Aluminum and Boron Ion Implantations into 6H-SiC Epilayers

TSUNENOBU KIMOTO, AKIRA ITOH, HIROYUKI MATSUNAMI, TOSHITAKE NAKATA,* and MASANORI WATANABE*

Department of Electronic Science and Engineering, Kyoto University, Yoshidahonmachi, Sakyo, Kyoto 606-01, Japan

Aluminum and boron ion implantations into n-type 6H-SiC epilayers have been systematically investigated. Redistribution of implanted atoms during high-temperature annealing at 1500°C is negligibly small. The critical implant dose for amorphization is estimated to be 1×10^{15} cm^{-2} for Al^+ implantation and 5×10^{15} cm^{-2} for B^+ implantation. By Al^+ implantation followed with 1500°C-annealing, p-type layers with a sheet resistance of 22 kΩ/□ can be obtained. B^+ implantation results in the formation of highly resistive layers, which may be attributed to the deep B acceptor level.

Key words: Electrical activation, ion implantation, Rutherford backscattering spectroscopy, silicon carbide

INTRODUCTION

Recent progress in crystal growth techniques of silicon carbide (SiC) has made the material a realistic candidate for high-power, high-temperature, and high-frequency devices.[1] In order to achieve the full potential of SiC, device processing technology such as oxidation, ion implantation, and metallization plays an important role. In particular, ion implantation is a key technique for selective doping in SiC, because a diffusion process is difficult due to the extremely low diffusion coefficients of impurities in SiC.

Through recent efforts in nitrogen ion (N^+) implantation into SiC,[2-5] reasonable sheet resistances (~800 Ω/□) and electrical activation (≥50%) could be achieved. However, ion implantation of acceptor-impurities into SiC is still immature. Regarding Al^+ implantation into SiC, there have been contradictions among the previous reports. Some groups succeeded in the formation of p-layer,[6,7] whereas the formation of highly resistive layers by the implantation was reported by other groups.[8,9] Besides, studies on B^+ implantation into SiC have been very limited.[7,8,10]

In this paper, the authors investigate Al and B ion implantations using device-quality n-type 6H-SiC epilayers. The implantation-induced damage and electrical properties of implanted layers are systematically characterized, together with the effects of implant dose and annealing temperature.

EXPERIMENTS

N-type 5 μm-thick 6H-SiC epilayers were grown by atmospheric-pressure chemical vapor deposition (CVD) on off-oriented 6H-SiC{0001} faces (step-controlled epitaxy). Substrates were n^+-type 6H-SiC with a net donor concentration of 2×10^{18} cm^{-3} (from Cree

*Ion Engineering Research Institute, Corporation, Tsuda, Hirakata, Osaka 573-01, Japan
(Received September 21, 1995)

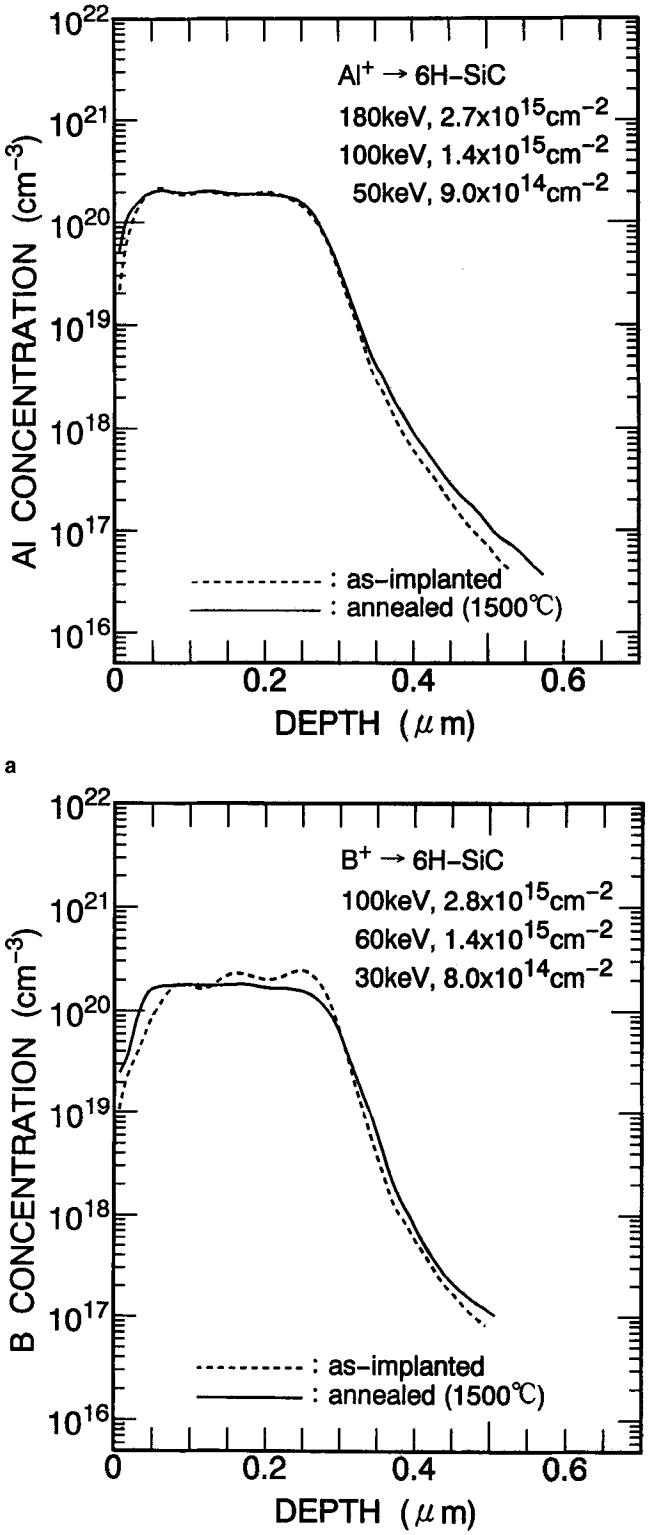

Fig. 1. (a) Al depth profiles before and after annealing at 1500°C for 30 min, and (b) B depth profiles before and after annealing at 1500°C for 30 min. Total implant dose is 5.0×10^{15} cm^{-2}.

Research Inc.). Epitaxial growth was carried out in a SiH_4-C_3H_8-H_2 system at 1500°C with a growth rate of 2.5 μm/h. The net donor concentration of epilayers was determined to be in the range of $7 \times 10^{15} \sim 2 \times 10^{16}$ cm^{-3} from capacitance voltage (C-V) measurements using Au/6H-SiC Schottky structures.

Table I. Al$^+$ and B$^+$ Implantation Conditions

Implanted Ion	Energy	Dose Ratio	Total Dose (cm^{-2})
Al$^+$	180 keV	0.54	$1 \times 10^{14} \sim 1 \times 10^{16}$
	100 keV	0.28	
	50 keV	0.18	
B$^+$	100 keV	0.56	$1 \times 10^{14} \sim 2 \times 10^{16}$
	60 keV	0.28	
	30 keV	0.16	

Al or B ions were implanted into the bare surface of samples at room temperature. The tilt angle between the ion beam direction and the ⟨0001⟩ axis was set 7° to avoid channeling effects.[5] In order to obtain box profiles, the triple implantation was performed, of which conditions are shown in Table I. The total implant dose was varied in the wide range of $1.0 \times 10^{14} \sim 1.0 \times 10^{16}$ cm^{-2} in Al$^+$ implantation and $1.0 \times 10^{14} \sim 2.0 \times 10^{16}$ cm^{-2} in B$^+$ implantation. The typical ion current density during implantation was 0.8 ~ 7 μA/cm^2. Post-implantation annealing was performed in a furnace heated by radio-frequency (rf) induction with a gas flow of Ar (1 atm). The annealing temperature and period were 1200 ~ 1500°C and 30 min, respectively. During the annealing, samples were set on a SiC-coated graphite susceptor.

The impurity-atom profiles were analyzed by secondary ion mass spectroscopy (SIMS) using a 14.0 keV O_2^+ primary beam. $^{30}Si^+$, $^{12}C^+$, $^{26}Al^+$, and $^{10}B^+$ were monitored in the SIMS measurements. The lattice damages of implanted layers were characterized by Rutherford backscattering spectroscopy (RBS) channeling measurements. RBS spectra were obtained using a 2.0 MeV He^{2+} beam with a scattering angle of 170°. The sheet resistance and resistivity were characterized by the van der Pauw method, and the average carrier concentration by Hall effect measurements. Al/Ti annealed at 950°C was used as ohmic contacts on implanted layers.

RESULTS AND DISCUSSION

Figure 1a shows Al-atom profiles before and after annealing at 1500°C for 30 min. The detailed implantation energies and doses are shown in the figure (total dose of Al$^+$: 5.0×10^{15} cm^{-2}). B-atom profiles, implanted with the same total dose, before and after annealing at 1500°C for 30 min are shown in Fig. 1b. Both the distributions exhibit box profiles of a peak concentration of 2×10^{20} cm^{-3}. By adjusting the implant energies, quite similar profiles could be obtained for Al$^+$ and B$^+$ implantations. The implantation depth can be estimated to be 0.5 ~ 0.6 μm. Redistribution of Al and B atoms is negligibly small after high-temperature annealing at 1500°C, though slight out-diffusion was observed in the B$^+$-implanted sample. Addamiano et al. reported that annealing at 1400°C causes serious out-diffusion of Al and B in implanted Lely crystals.[11] This disagreement may originate from

the difference in quality of used crystals. The Lely crystals, which are grown at very high temperature of 2400°C, may contain high density of vacancies and/or interstitials, which enhance the diffusion of impurities during heat treatment.

Figure 2 shows the RBS spectra obtained from (a) Al⁺-implanted and (b) B⁺- implanted samples with a total dose of 1.0×10^{15} cm^{-2}. In the figures, aligned spectra of as-implanted and 1500°C-annealed samples together with a random spectrum are shown. For comparison, the aligned spectrum from a virgin sample is also shown. Here, annealing at 1500°C was mainly employed, because the backscattering yield at the Si edge in aligned geometry decreased with the increase in annealing temperature. In Al⁺ implantation (Fig. 2a), an almost randomized layer with a thickness of 0.4 μm thickness is formed at the surface. In B⁺ implantation (Fig. 2b), however, the as-implanted layer has crystalline structure. After the samples

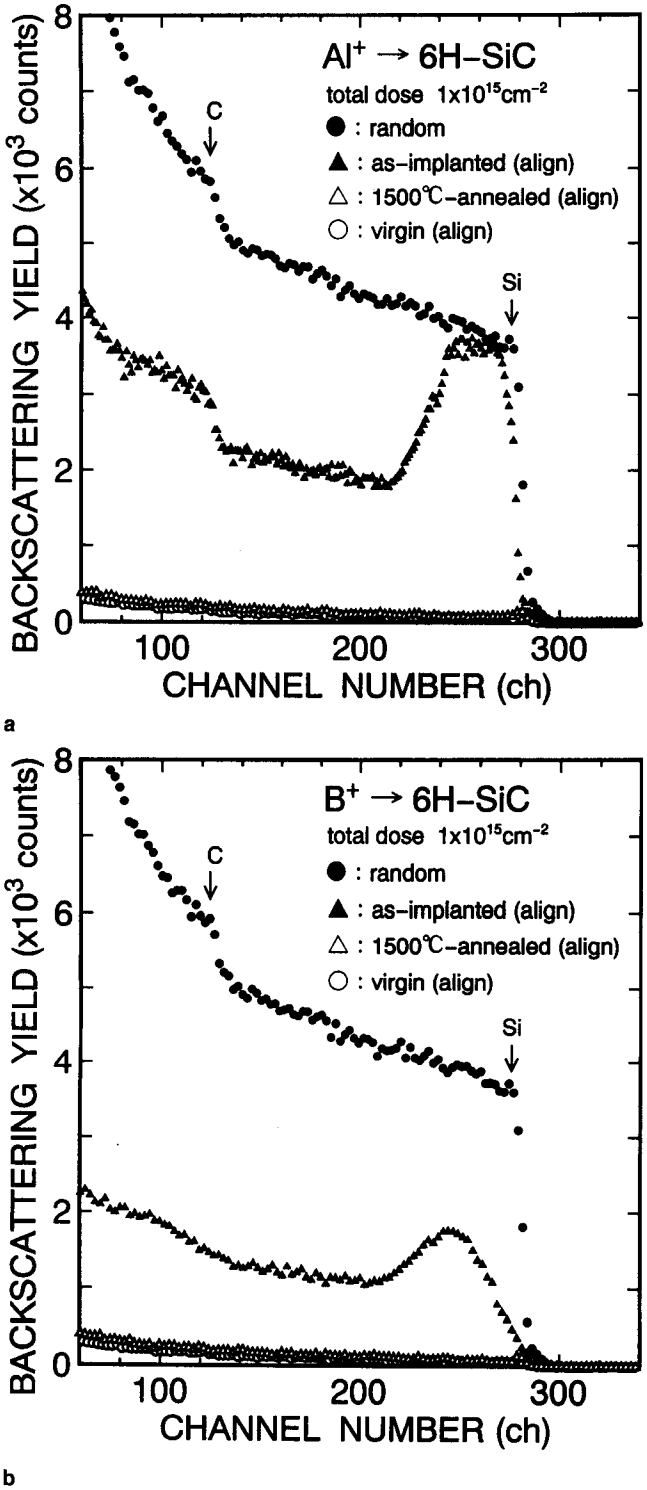

Fig. 2. RBS spectra obtained from (a) Al⁺-implanted and (b) B⁺-implanted samples with a total dose of 1.0×10^{15} cm^{-2}. In the figures, aligned spectra of as-implanted and 1500°C-annealed samples together with a random spectrum are shown. For comparison, the aligned spectrum from a virgin sample is also shown.

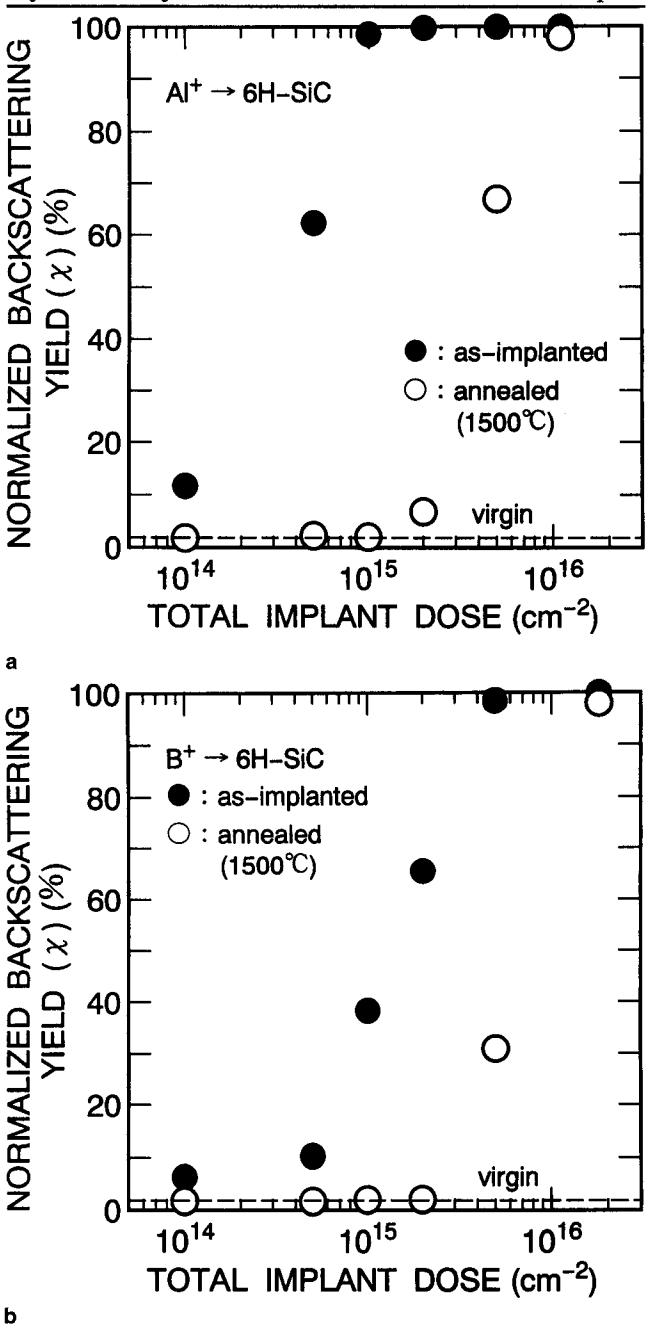

Fig. 3. (a) Al⁺ implant dose dependence of normalized backscattering yield in RBS spectra for as-implanted and 1500°C-annealed samples, and (b) B⁺ implant dose dependence of normalized backscattering yield in RBS spectra for as-implanted and 1500°C-annealed samples.

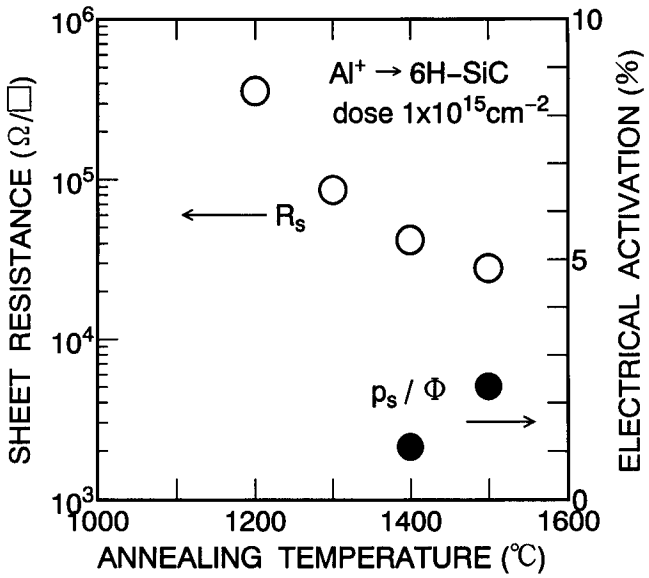

Fig. 4. Annealing temperature dependence of sheet resistance and electrical activation ratio for Al+-implanted layers. Total implant dose is 1.0×10^{15} cm^{-2}.

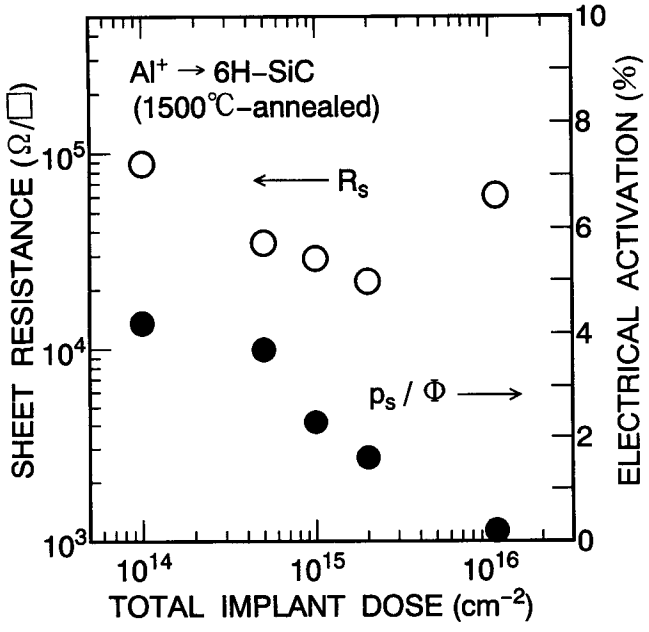

Fig. 5. Implant dose dependence of sheet resistance and electrical activation ratio for Al+-implanted layers annealed at 1500°C.

were subjected to high-temperature annealing at 1500°C, the lattice damages are significantly reduced in both the cases, though the backscattering yields from annealed samples are slightly higher than that from a virgin sample.

The difference in damages between Al+- and B+-implanted layers is clearly manifested in Fig. 3, where the implant dose dependence of the normalized backscattering yield in RBS spectra for as-implanted and 1500°C-annealed samples are shown. Here, the normalized backscattering yield (χ) was defined as the average yield from implanted layers (0.05 ~ 0.40 μm depth) in an aligned geometry normalized by the random yield. The normalized backscattering yield for as-implanted layers represents a steep increase at about 5×10^{14} cm^{-2} dose in Al+ implantation (Fig. 3a), and 1×10^{15} cm^{-2} dose in B+ implantation (Fig. 3b). From Fig. 3, the critical implant dose for complete amorphization can be estimated to be 1×10^{15} cm^{-2} in Al+ implantation, and 5×10^{15} cm^{-2} in B+ implantation. The lower critical implant dose in the former case indicates that the implantation-induced damages are more severe in Al+ implantation. This result reflects the difference in the mass of implanted ions: Al atoms are much heavier, which leads to dominant collisions of implanted ions with nuclei of a host material.[12] In the present study, we formed the almost same implantation profiles between Al+ and B+ implantations. The heavier mass of Al atoms requires higher-energy implantation to obtain a profile with the same junction depth, owing to its smaller projected ranges. This high-energy implantation is another reason why the lattice damages are more severe in Al+ implantation. After annealing at 1500°C, the damages are significantly removed when the as-implanted layers have crystalline structures as shown in Fig. 3. However, the severe damages remain even after annealing, once complete amorphous layers are formed through implantation, which is quite similar to the case of N+ implantation.[4] For further investigation on lattice damages, cross-sectional transmission electron microscope (TEM) observation is required.

From cross-sectional scanning electron microscope (SEM) observation of implanted samples, the junction depth was estimated to be 0.60 μm for Al+- and B+-implanted samples after annealing, which is in good agreement with SIMS measurements (Fig. 1).

Figure 4 shows the annealing temperature dependence of sheet resistance and electrical activation ratio for Al+-implanted layers. The total implant dose is 1.0×10^{15} cm^{-2}. Here, the electrical activation ratio was defined as the ratio of the sheet carrier concentration p_s (p_s = pd, p: the average carrier concentration, d: the junction depth) to the Al+ dose Φ. The carrier concentration should be considerably lower than the concentration of Al acceptors substituting Si-sublattice sites because of the large ionization energy (~250 meV)[13] of Al acceptors in SiC. Although C-V measurements using Hg-probe or Hall effect measurements at high temperatures are required to clarify the Al acceptor concentration in implanted layers, the definition described above may be useful for device applications. The annealing at 1200°C is not enough for the activation of implanted Al: The implanted layer had a very high sheet resistance of 360 kΩ/□, and Hall effect measurements were technically difficult due to very high resistance between the contacts. With increasing annealing temperature, the sheet resistance was reduced, and the electrical activation was improved. After annealing at temperatures higher than 1400°C, Al+-implanted layers showed clear p-type conduction. The sheet resistance of a 1500°C-annealed sample (28 kΩ/□) is a little higher than a theoretical value (16 kΩ/□) estimated from the implant dose (1.0×10^{15} cm^{-2}), the junction depth (0.60 μm), the ionization energy of Al acceptors (250 meV),

and a hole mobility (20 cm^2/Vs), with an assumption that all the implanted Al atoms substitute lattice sites. The corresponding electrical activation ratio is 2.4%, due to the large ionization energy of Al acceptors.

Figure 5 shows the dose dependence of the sheet resistance and electrical activation ratio of Al^+-implanted layers. The annealing was performed at 1500°C for 30 min. The sheet resistance gradually decreases with the increase of Al^+ dose in the range of 1.0×10^{14} $cm^{-2} \sim 2.0 \times 10^{15}$ cm^{-2}, and a sheet resistance of 22 kΩ/□ was obtained with an electrical activation ratio of 1.6%. For a sample implanted with a 1.0×10^{16} cm^{-2} dose, the implanted layer was rather resistive, which may be caused by the severe implantation damage as shown in Fig. 3a. The electrical activation ratio decreased when the total implant dose exceeds 1.0×10^{15} cm^{-2}, probably due to remaining damages. In N^+ implantation into SiC, relatively low sheet resistances of 770 ~ 840 kΩ/□ have been achieved.[3-5] The high sheet resistances of Al^+-implanted layers come from the low electrical activation ratio caused by the deep Al acceptor level and the low hole mobility (about 1/5 ~ 1/10 of electron mobility). To reduce the sheet resistance, the Al^+ dose should be increased, keeping the implantation-induced damages as small as possible. In this sense, hot-implantation may be promising.[7]

Recently, Rao et al. reported a systematic study on Al^+ and B^+ implantations into 6H-SiC.[7] According to the report, Al^+ implantation at room temperature resulted in the formation of n-type or resistive layers and p-type layers could be obtained only by hot implantation at 850°C followed by annealing at 1400°C. Although the origins of discrepancy between their result and the present one are not clear, one possible reason may be the difference in annealing processes. In sample annealing, Rao et al. used a conventional electric furnace, whereas we employed a rf-induction heated furnace, which allows very fast temperature rising (≥40°C/s). This rapid heating might prevent unfavorable annealing stages of defect formation at low temperatures.

On the other hand, B^+-implanted layers were highly resistive which disturbed the clear identification of conduction type (p or n) as well as the accurate measurement of electrical activation. Figure 6 shows the implant dose dependence of resistivity for B^+-implanted layers annealed at 1500°C. The dotted line denotes the dependence calculated from the B acceptor ionization energy (350 meV)[14,15] and a mobility of 20 cm^2/Vs. The obtained resistivities (15 ~ 120 Ωcm) agree with predicted values. We confirmed that the resistivities of implanted layers almost coincide with those of B-doped epilayers with the similar B concentrations.

Thus, we believe that the high resistivities of B^+-implanted layers are not due to remaining damages but inherent to B-doped SiC because of its deep acceptor level. It has been suggested that B atoms can occupy both Si- and C-lattice sites.[16,17] The former

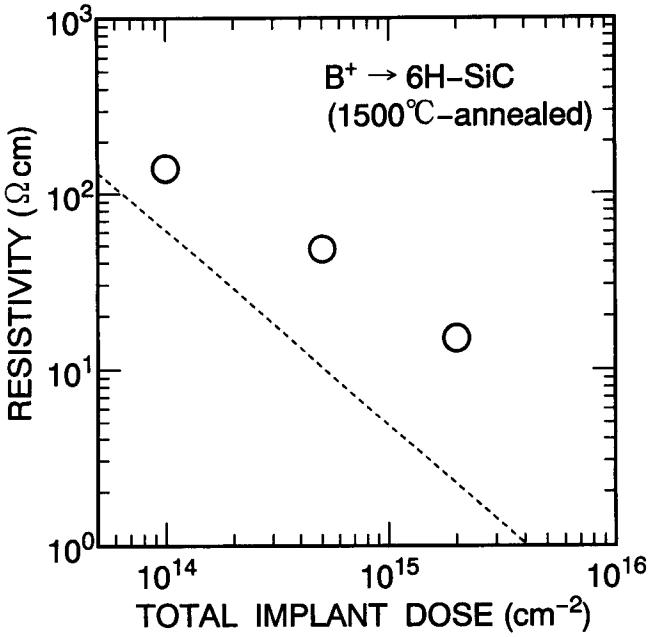

Fig. 6. Implant dose dependence of resistivity for B^+-implanted layers annealed at 1500°C. The dotted line denotes the dependence calculated from the B acceptor ionization energy (350 meV) and a mobility of 20 cm^2/Vs.

forms an acceptor with an ionization energy of 0.3 ~ 0.4 eV, and the latter forms a so-called D-center with an activation energy of 0.6 ~ 0.7 eV.[15-17] To clarify the occupation sites of implanted B atoms, deep level transient spectroscopy (DLTS) and photoluminescence are required.

B^+ implantation may be effective to form highly resistive layers rather than to make p^+ well. For example, the edge termination of high-voltage Schottky rectifiers is a hopeful application of B^+ implantation.[18]

CONCLUSION

We systematically investigated Al^+ and B^+ implantations into n-type 6H-SiC epilayers. Redistribution of implanted atoms during high-temperature annealing at 1500°C was negligibly small. The implantation-induced damages were more severe in Al^+ implantation due to the larger mass of implanted ions. The critical implant dose for amorphization was estimated to be 1×10^{15} cm^{-2} for Al^+ implantation and 5×10^{15} cm^{-2} for B+ implantation. Even in low-dose implantation, annealing at high temperatures led to higher electrical activation of implanted atoms. By Al^+ implantation followed by 1500°C-annealing, p-type layers with a sheet resistance of 22 kΩ/□ could be obtained. B^+ implantation resulted in the formation of highly resistive layers, which may be mainly attributed to the deep B acceptor level.

ACKNOWLEDGMENT

This work was partially supported by New Energy and Industrial Technology Development Organization. The authors are grateful to Professor N. Imanishi and Dr. K. Yoshida in Department of Nuclear Engineering, Kyoto University, for the use of RBS equip-

ment. They also express their thanks to Mr. N. Inoue of Kyoto University for his technical assistance.

REFERENCES

1. *Silicon Carbide and Related Materials*, eds. M.G. Spencer, R.P. Devaty, J.A. Edmond, M.A. Khan, R. Kaplan and M.M. Rahman (Bristol: Institute of Physics, 1994).
2. G. Pensl, R. Helbig, H. Zhang, G. Ziegler and P. Lanig, *Mater. Res. Soc. Symp. Proc.* 97, 195 (1987).
3. M. Ghezzo, D.M. Brown, E. Downey, J. Kretchmer, W. Hennessy, D.L. Polla and H. Bakhru, *IEEE Electron Dev. Lett.* 12, 639 (1992).
4. T. Kimoto, A. Itoh, H. Matsunami, T. Nakata and M. Watanabe, *J. Electron. Mater.* 24, 235 (1995).
5. S. Yaguchi, T. Kimoto, N. Ohyama and H. Matsunami, *Jpn. J. Appl. Phys.* 34, 3036 (1995).
6. E.V. Kalinina, N.K. Prokof'eva, A.V. Suvorov, G.F. Kholuyanov and V.E. Chelnokov, *Sov. Phys. Semicond.* 9, 820 (1976).
7. M.V. Rao, P. Griffiths, O.W. Holland, G. Kelner, J.A. Freitas, Jr., D.S. Simons, P.H. Chi and M. Ghezzo, *J. Appl. Phys.* 77, 2479 (1995).
8. O.J. Marsh, *Silicon Carbide 1973*, eds. R.C. Marshall, J.W. Faust, Jr. and C.E. Ryan, (Columbia: Univ. of South Carolina Press, 1974), p.471.
9. J.A. Edmond, S.P. Withrow, W. Wadlin and R.F. Davis, *Mater. Res. Soc. Symp. Proc.* 77, 193 (1987).
10. M. Ghezzo, D.M. Brown, E. Downey, J. Kretchmer and J.J. Kopanski, *Appl. Phys. Lett.* 63, 1206 (1993).
11. A. Addamiano, G.W. Anderson, J. Comas, H.L. Hughes and W. Lucke, *J. Electrochem. Soc.* 119, 1355 (1972).
12. H. Ryssel and I. Ruge, *Ion Implantation* (Chichester: John Wiley & Sons, 1986), Ch. 2.
13. M. Ikeda, H. Matsunami and T. Tanaka, *Phys. Rev.* B22, 2842 (1980).
14. Yu.A. Vodakov, N. Zhumaev, B.P. Zverev, G.A. Lomakina, E.N. Mokhov, V.G. Oding, V.V. Semenov and Yu.F. Simakhin, *Sov. Phys. Semicond.* 11, 214 (1977).
15. W. Suttrop, G. Pensl and P. Lanig, *Appl. Phys.* A51, 231 (1990).
16. A.O. Konstantinov, *Sov. Phys. Semicond.* 26, 151 (1992).
17. W.J. Choyke and G. Pensl, private communication.
18. A. Itoh, T. Kimoto and H. Matsunami, *Proc. 7th Intl. Symp. Power Semicond. Devices & IC's* (Yokohama, 1995), p.101.